

Removal Efficiency of Lipid-regulating Drug Clofibrac Acid from the Aquatic Environment by Calcined Anionic Clay ZnAl-CO₃



<https://doi.org/10.15255/CABEQ.2020.1797>

E. Mourid, M. Lakraimi,* L. Benaziz, and M. Cherkaoui

Physical Chemistry of Materials Team,
Cadi Ayyad University, Marrakech, Morocco

Original scientific paper
Received: March 28, 2020
Accepted: July 14, 2020

Clofibrac acid (CA) is widely used as regulator of lipid levels in blood; it is considered one of the residual drugs that have a high persistence in the aquatic environment. After wastewater treatment, only a small amount of CA can be removed. The aim of this work was to investigate the reduction of CA in contaminated wastewater using calcined anionic clay ZnAl-CO₃, which was chosen for its higher adsorption capacity, recyclability, and non-regeneration of sludge. The maximum retention amount, Q_m , exceeded 2220 mg g⁻¹, and the value of ΔH° suggested a physical process. The removal rate achieved 90 %, and the remaining quantity was widely below the tolerance thresholds. Retention was achieved by hydrogen bonds and electrostatic interactions between the adsorbate molecules. Recycling tests clearly suggested that this material is recyclable, promising, and very effective compared to other adsorbents. This retention contributes to the attenuation of persistent lipid regulator.

Keywords:

anionic clay, clofibrac acid, persistence, elimination, recycling

Introduction

Over the past few years, there has been growing concern about drugs due to their widespread use, continued release, and further evidence of negative environmental effects¹. Among the emerging micropollutants, pharmaceuticals have attracted the interest of researchers worldwide for several years. Many reports on the effects and risks of these compounds have been revealed to raise awareness around the toxicity of such pollutants². In addition, these compounds are directly emitted in rivers without effluent treatment.

At this moment, about 100 types of personal care products have been detected in rivers^{3–6}, lakes⁷, oceans^{8,9}, and groundwater¹⁰. Some products may have a toxic effect on aquatic organisms and even on humans^{11,12}.

Clofibrac acid has the chemical name 2-(4-chlorophenoxy)-2-methyl-propanoic acid, its sorption coefficient ($\log K_{ow}$) in the order of 0.9, 1.36, and 1.88, and its melting point is between 120 °C–122 °C¹³. It is widely used as an active ingredient in blood lipid regulators clofibrate, etofyllinclofibrate and etofibrate. It is a resistant drug to biodegradation and has a very strong persistence in the environment¹⁴. The blood lipid regulator consumption is very high, about thousands of tons per year

have been intended for therapeutic care in cases of angiocardopathy problems⁸. Its first detection was reported in samples from wastewater treatment plants in America in the 1930s¹⁵. Nowadays, CA is considered one of the residual drugs with persistence in the environment estimated at 21 years. It is frequently detected in the global environmental monitoring of plant protection products^{15,16}. During a typical pass through wastewater treatment in factories, only 40 %–50 % of the initial amount of CA is effectively removed^{17,18}. Thus, several methods have been used in recent years for the removal of pharmaceutical products from wastewater, such as advanced oxidation processes, photodegradation, biological treatments, adsorption, etc.^{19–28}

This work aimed to reduce the drug contamination of wastewater, such as that of blood lipid regulators, in order to reduce their persistence in the aquatic environment. Therefore, the removal of CA from wastewater was studied using a calcined anionic clay ZnAl-CO₃ material (CLDH) still based on the reconstruction of LDH phases intercalated by this drug. The objective was to optimise the amount of retention and the rate of elimination of this pollutant while optimising various experimental parameters, such as contact time, pH of retention environment, initial concentration of the drug, and CA/CLDH mass ratio. A comparative study allowed us to evaluate the retention capacity of CLDH relative to those of other adsorbents given in the litera-

*Corresponding author: mlakraimi@yahoo.fr

ture. In addition, the possibility of regeneration of the used material was studied while examining the variation of its retention capacity as a function of the regeneration cycles. Layered double hydroxides (LDHs) or anionic clays, and their calcined products (CLDHs), have been widely used as degradation photocatalysts or as adsorbent of a wide variety of micropollutants^{29–32}. Several studies have evoked the elimination of this pollutant using adsorbents, such as plants, clays, activated carbon, chitosan, and resins^{13,33–36}. Most of these studies have not explored the possibilities of recycling and regenerating their materials with regard to this pollutant, or compared their results concerning the capacity and rate of adsorption with those of other adsorbents while optimising the various factors influencing elimination. For these reasons, the originality of this work lies in the optimisation of the experimental parameters that could lead to high retention capacities and maximum removal rates, the recycling study of the chosen adsorbent material based on zinc and aluminium to minimise the cost of removing the pollutant, and a comparative study with other recent work in order to situate the effectiveness of the used material compared to other adsorbents.

The retention process of the pollutant is confirmed by several techniques, such as X-ray diffraction (XRD), infrared spectroscopy (IR), scanning electron microscopy (SEM), and thermogravimetric analysis (TGA/DTG).

Materials and methods

Preparation of ZnAl-CO₃ adsorbent material

The adsorbent anionic clay ZnAl-CO₃ was synthesized by coprecipitation method at a constant pH of 10. It was prepared from metallic salts solutions AlCl₃·6H₂O (0.4 mol L⁻¹, purity ≥ 98 %), Zn(SO₄)·7H₂O (0.4 mol L⁻¹, purity ≥ 98 %), basic solution of Na₂CO₃ (0.3 mol L⁻¹, purity ≥ 99.5 %), and NaOH (0.1 mol L⁻¹, purity ≥ 98 %). The metallic ratio Zn/Al is 2. The obtained precipitate was intercalated only by carbonate anions (CO₃²⁻) because their affinity towards LDH interlayer is very high compared to other anions³⁷. The synthesized product was dried at room temperature (25 °C) for 2 days, and calcined at 500 °C for 5 hours, leading mainly to mixed oxides. These led to the reconstruction of an LDH phase after their rehydration in a solution containing the CA pollutant anions.

Retention experiments

Adsorption of the drug CA by CLDH was investigated in a batch system at room temperature (25 °C) with constant contact time (2 h), and constant pH by addition of HCl (0.1 mol L⁻¹) or NaOH

(0.1 mol L⁻¹), with nitrogen bubbling. The experiments were carried out by dispersion of adsorbent CLDH (10, 30, or 50 mg) in solutions of 100 mL containing CA in different concentrations (from 10 to 500 mg L⁻¹). After contact time and filtration, the solids obtained were dried, and analysed by XRD, IR, TGA/DTG and SEM. The filtrate was analysed by UV-Vis spectroscopy at 275 nm, which is the universally accepted technique for the detection of CA concentration³⁸. The capacity of adsorption was determined by Eq. (1):

$$Q = \frac{(C_i - C_e) \cdot V}{m} \quad (1)$$

where Q represents the amount of CA retained by the adsorbent material, C_i is the initial concentration and C_e the equilibrium concentration of CA, and m is the mass of CLDH in volume V .

For the thermodynamic study, the same adsorption process was followed under optimal conditions as a function of time in a thermostatic bath, in order to regulate the desired temperature. The temperatures of 298 K, 318 K, and 333 K were chosen. When adsorption was completed for each of the three temperatures, the solutions were filtered, and the residual concentration of CA in the filtrate was determined in order to calculate the adsorption capacity Q .

Structural characterisation techniques

The XRD measurements were performed on an XPERT-PRO powder diffractometer, equipped with a copper anticathode tube ($\lambda = 0.15415$ nm) and a graphite-blade back monochromator. The diffractograms were measured in the range 3°–70° in 2θ , and step counting time was 41 s.

Measurements by infrared spectroscopy were obtained using a JASCO Fourier transform spectrometer model FT/IR-4600. The samples were analysed by transmission method in a range of wavenumbers between 400 and 4000 cm⁻¹. The resolution was 4 cm⁻¹ and the number of scans was 20.

Scanning Electron Microscopy (SEM) allows visualisation of the external morphology of materials. The analysis of the external surface of the material was carried out using a TESCAN VEGA 3 LM apparatus. The observations were made under a voltage of 10 kV.

The thermograms were recorded using a SETARAM TGA/DTG microbalance 92 allowing operation under a controlled atmosphere, in this case in air, and simultaneously performing thermogravimetry and differential thermal analysis. The temperature was raised from 25 °C to 800 °C with a heating rate of 5 °C min⁻¹. The tests were carried out on powder quantities of an initial mass of 12 mg contained in alumina crucibles.

Results and discussion

Characterisation of ZnAl-CO₃

The different analyses of the ZnAl-CO₃ adsorbent material and its calcined phase, by X-ray diffraction, IR spectroscopy, thermogravimetry and scanning electron microscopy are presented in Fig. 1. Fig. 1a indicates that the obtained phase is comparable to that of natural hydrotalcite³⁹, it shows a good crystalline organisation of this phase. The majority of the lines are thin, symmetrical, and intense. All the diffraction lines observed are indexed in a hexagonal system of rhombohedral symmetry (space group R $\bar{3}m$). The angular position of the first line (003) gives direct access to the interlayer distance ($c/3 = d_{003}$). Another interesting diffraction peak located near 61° in 2θ is indexed. It is related

to the metal-metal interatomic distance in the sheet, according to the relation $a = 2 d_{110}$. The presence of lines around 61° in 2θ (line (110)) confirms the existence of a well crystallised LDH phase⁴⁰, the lattice parameters are $a = 0.306$ nm, $c = 2.292$ nm, and $d = 0.764$ nm.

The thermogram (Fig. 1b) is similar to that of a natural hydrotalcite. At 80 °C, there is a slight loss that could correspond to the elimination of water weakly bound to the surface. However, the loss that occurs between 80 °C and 190 °C, which is around 13 %, is due to the elimination of interlamellar water. The decomposition of carbonate anions into CO₂ occurs from 190 °C at the same time as dehydroxylation⁴¹.

The IR spectrum (Fig. 1c) of the phase intercalated by the carbonate anions shows bands around 1630 and 3470 cm⁻¹ corresponding respectively to

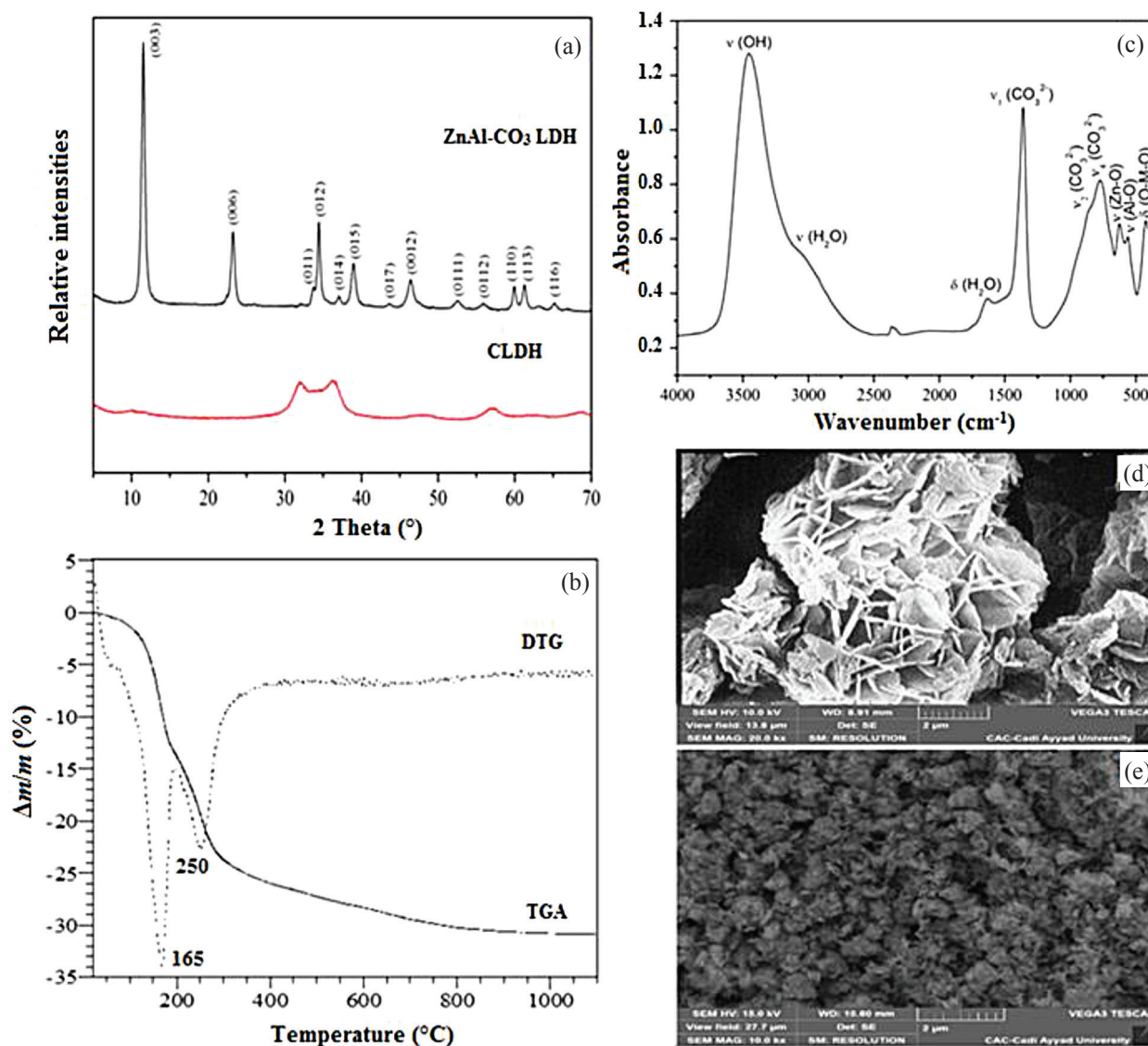


Fig. 1 – Powder XRD patterns of LDH and CLDH (a), TG-DTG curves (b), IR spectrum (c), SEM photographs of LDH (d), and CLDH (e)

the deformation vibrations of the interlayer water molecules δ (H_2O), and to the valence vibrations of the hydroxyl groups of the brucite layers ν (O-H). The characteristic bands with carbonate anions are between 879 and 1480 cm^{-1} . Finally, we also note the presence of metal-oxygen vibrations with a band at 554 cm^{-1} for Al-O, and a band at 615 cm^{-1} for Zn-O⁴². The band around 400 cm^{-1} corresponds to the deformation vibrations of O-M-O^{43,44}.

The SEM photographs are presented in Fig. 1d and Fig. 1e. For the ZnAl- CO_3 phase (Fig. 1d), the lamellar structure of the compound is perfectly demonstrated by the presence of crystallites, which are distributed homogeneously in the form of sand rose. On the other hand, in the SEM image corresponding to the calcined phase (Fig. 1e); there is the disappearance of the lamellar character, which may be due to the destruction of the LDH sheets and the appearance of aggregates probably corresponding to mixed oxides.

Characteristics of the CA pharmaceutical drug

Clofibrac acid ($\text{C}_{10}\text{H}_{11}\text{ClO}_3$; 99 % of purity) has a molecular weight of 214.65 g mol^{-1} , it was purchased from Acros Organics grade, its pK_a value is 2.5, and its solubility in water is 582.5 mg L^{-1} at $25\text{ }^\circ\text{C}$. This drug is considered an active metabolite of clofibrate and a lipid-lowering active ingredient. It allows reduction of blood lipid levels and acts against the excess of cholesterol¹³.

Effect of pH

The pH of the solution is a factor that can modify the surface charge of the adsorbent material and the distribution of speciation of the adsorbate in solution. The variation of the retained quantity of

CA by CLDH as a function of the pH is presented in Fig. 2a. The initial concentration of CA used was 20 mg L^{-1} with 30 mg of adsorbent. The solutions were stirred for 2 hours at room temperature ($25\text{ }^\circ\text{C}$).

It should be noted that maximum retention occurs at pH value of 5 by means of the electrostatic interactions and/or the hydrogen bonds, which take place between the COO^- group of the CA and the hydroxyl group of the reconstructed LDH layers. CA is a relatively weak acid; an increase in pH from 5 to 6 promotes its dissociation (Fig. 2b) with an increase in its solubility, which leads to an increase in the retention capacity.

For values of $\text{pH} < 5$, the decrease in CA retention can be explained by partial dissolution of the matrix by hydrolysis, and/or probably by protonation of CA, which leads to the existence of repulsive interactions between OH group of the reconstructed LDH sheet and the COOH group of the CA⁴⁵.

The gradual decrease in the retained amount of CA between pH 7 and pH 11 can only be explained by relative contamination with CO_3^{2-} , which has a high affinity for LDH³⁰. This may also be due to the presence of dissociated CA molecules with higher solvation energy. In this case, the solvation sphere becomes more rigid, and the diffusion of solvated CA between the layers of the material will be more difficult³⁵. The following experiments in this work were carried out at pH 5.

Kinetic study

The contact of CA suspension with CLDH results in an interaction and as time passes, the adsorbed amount increases. To determine the equilibrium time when retaining CA by CLDH, the kinetic study was performed for two initial concentrations

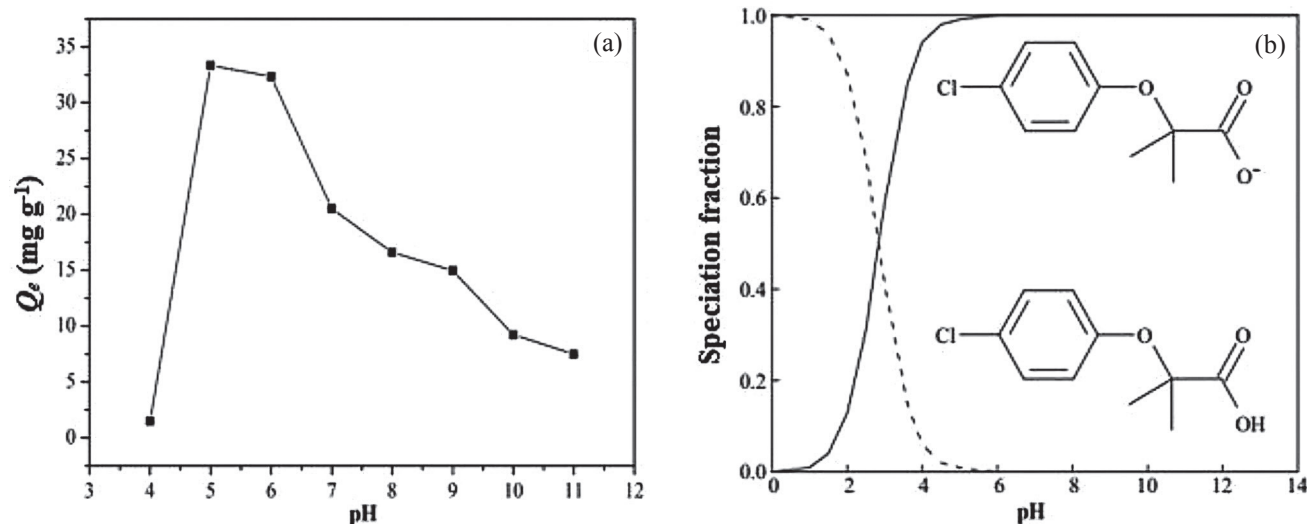


Fig. 2 – Quantities of CA retained by 30 mg CLDH as a function of pH (a), and speciation diagram of CA⁴⁵(b)

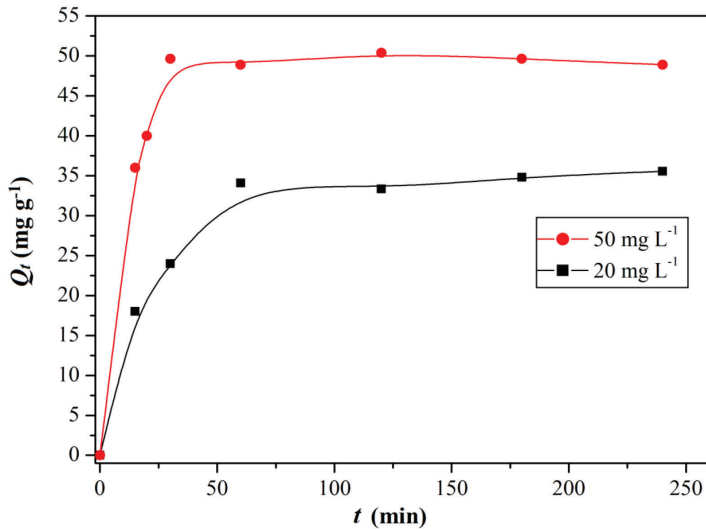


Fig. 3 – Kinetics of retention of CA by 30 mg of CLDH at initial concentrations (20 mg L^{-1} and 50 mg L^{-1})

of CA (20 mg L^{-1} and 50 mg L^{-1}) with 30 mg of CLDH and contact times from 0 to 4 hours. For each initial concentration, the evolution of the amount of retained CA versus contact time is shown in Fig. 3.

The obtained results showed that the adsorption process was relatively fast, the equilibrium was reached after one hour for the two concentrations of CA. For the initial concentrations of 20 mg L^{-1} and 50 mg L^{-1} , the maximum quantities retained Q_m were 36 mg g^{-1} and 50 mg g^{-1} , respectively. The process is described by the rehydration of the mixed oxides in CA solution, which leads to the formation of hydroxyl groups of the brucitic sheets, and consequently, the reconstruction of an LDH phase via the conserved memory effect of the initial LDH phase. That is, the CA anions interact simultaneously with the surface sites and those between the reconstructed LDH sheets.

Intraparticle diffusion, pseudo-first and pseudo-second order models were used to describe and examine this kinetic process.

Pseudo-first and pseudo-second order models

Kinetic retention gives some information about the affinity between the adsorbate and the adsorbent, and defines the efficiency of adsorption. The linearisation by the pseudo-first and pseudo-second order models are given by Eqs. (2) and (3)⁴⁶:

$$\log(Q_e - Q_t) = \log Q_e - k_1 \cdot t \quad (2)$$

$$\frac{t}{Q_t} = \frac{1}{k_2 \cdot Q_e^2} + \frac{1}{Q_e} \cdot t \quad (3)$$

where Q_e is the retention quantity at equilibrium, and Q_t is the retention quantity at time t , k_1 and k_2 are the rate constants of the pseudo-first and pseudo-second order models of adsorption.

From the results collected in Table 1 and from the values of R^2 , as well as by comparison of the experimental and theoretical retained amounts, it could be said that the retention kinetics of CA by CLDH is in good agreement with the pseudo-second order model, which suggests that the retention of the adsorbate on the material surface is fast.

Intraparticle diffusion model

The intraparticle diffusion model provides some information on the mode of solute transfer from the liquid phase to the solid phase; it also investigates the contribution of intraparticle behaviour on the adsorption mechanism. This model can be described by the following equation⁴⁷:

$$Q_t = K_{ip} \cdot t^{1/2} + C \quad (4)$$

where Q_t is the amount of retention (mg g^{-1}), K_{ip} is the intraparticle diffusion rate constant ($\text{mg g}^{-1} \text{ min}^{-1/2}$), and C is the capacity of the boundary layer.

The plot of Q_t versus $t^{1/2}$ (Fig. 4) led to the appearance of two linearities for both concentrations (20 mg L^{-1} and 50 mg L^{-1}). The first (phase I) corresponded to the adsorption of CA on the surface of reconstructed LDH followed by the second, which

Table 1 – Parameters of the pseudo-first and pseudo-second order models and the maximum adsorption amounts of CA by CLDH

| Pseudo-first order | | | | | |
|---------------------------------|--|--|--|---|-------|
| C_0 (mg L^{-1}) | Equation | k_1 (h^{-1}) | $Q_{e \text{ th}}$ (mg g^{-1}) | $Q_{e \text{ exp}}$ (mg g^{-1}) | R^2 |
| 20 | $\log(Q_e - Q_t) = -0.005 \cdot t + 1.018$ | 0.005 | 2.77 | 36 | 0.668 |
| 50 | $\log(Q_e - Q_t) = -0.003 \cdot t + 0.635$ | 0.003 | 1.89 | 50 | 0.289 |
| Pseudo-second order | | | | | |
| C_0 (mg L^{-1}) | Equation | k_2 ($\text{g mg}^{-1} \text{ h}^{-1}$) | $Q_{e \text{ th}}$ (mg g^{-1}) | $Q_{e \text{ exp}}$ (mg g^{-1}) | R^2 |
| 20 | $t/Q_t = 0.027 \cdot t + 0.256$ | 0.003 | 37 | 36 | 0.996 |
| 50 | $t/Q_t = 0.020 \cdot t + 0.040$ | 0.010 | 49.7 | 50 | 0.999 |

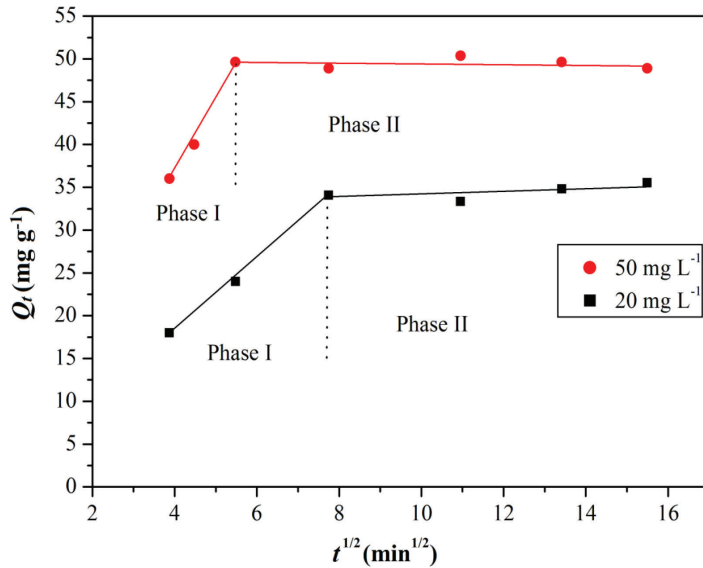


Fig. 4 – Linear representation of the kinetic model of intraparticle diffusion for CA

corresponded to a state of saturation (phase II). This result indicated the speed of the adsorption process. The contact between LDH and CA was achieved by the presence of hydrogen bonds and electrostatic interactions between the hydroxyl (OH) groups of the reconstructed LDH sheets and the carboxylate groups of the pollutant.

The different constants resulting from intraparticle scattering are shown in Table 2.

The R^2 values indicated that diffusion was not a limit step for this retention. Different interpretations have been put forward concerning the application of the intraparticle diffusion model, in which the diffusion of particles is not the only limiting step, because of the presence of other processes, such as external mass transfer and surface diffusion or the combination of both. The diffusion of the solute

from the liquid phase towards the interior of the adsorbent can be neglected, in this case, the surface adsorption was a dominant step^{48,49}. There were two stages in the adsorption process. The first part concerned the adsorption on the external surface or the instantaneous adsorption, the second part corresponded to the equilibrium state, where the intraparticle diffusion was slow probably because of the adsorption sites saturation⁵⁰.

Thermodynamic study

The study of the influence of temperature on the adsorption of the drug product was carried out with three temperatures of 298, 318, and 333 K, in intervals of 10 to 120 minutes. The concentration of the CA drug was maintained at 50 mg L⁻¹, and the mass of the calcined LDH was 30 mg. Thermodynamic parameters, namely enthalpy (ΔH°), Gibbs free energy (ΔG°), and entropy (ΔS°) were calculated from the following equations⁵¹:

$$K_c = \frac{Q_e}{C_e} \quad (5)$$

$$\ln K_c = \frac{\Delta S^\circ}{R} - \frac{\Delta H^\circ}{RT} \quad (6)$$

$$\Delta G^\circ = -RT \cdot \ln K_c \quad (7)$$

where Q_e is the amount of adsorption (mg g⁻¹), K_c the distribution coefficient, C_e the concentration of CA at equilibrium (mg L⁻¹), R (8.314 J mol⁻¹ K⁻¹) is the ideal gas constant, and T (K) is the adsorption temperature. The values of thermodynamic parameters ΔH° and ΔS° were determined according to the linear plot of $\ln K_c$ versus $1/T$. The different thermodynamic parameters are presented in Table 3. It appeared that the values of ΔG° were negative, indicating that the adsorption of this drug onto CLDH was governed by a spontaneous process, the nega-

Table 2 – Parameters of intraparticle diffusion model for adsorption of CA by CLDH

| Phase I | | | | Phase II | | |
|--------------------------------|---|--------------------------------|-------|---|--------------------------------|-------|
| C_0 (mg L ⁻¹) | K_{1d} (mg g ⁻¹ min ^{-1/2}) | C_1 (mg g ⁻¹) | R^2 | K_{2d} (mg g ⁻¹ min ^{-1/2}) | C_2 (mg g ⁻¹) | R^2 |
| 20 | 4.17 | 1.60 | 0.998 | 2.28 | 31.90 | 0.884 |
| 50 | 8.61 | 2.21 | 0.992 | 2.72 | 49.68 | 0.871 |

Table 3 – Thermodynamic parameters obtained from kinetic adsorption of CA onto CLDH

| T (K) | E_a (kJ mol ⁻¹) | K_c (L g ⁻¹) | $\ln K_c$ | ΔG° (kJ mol ⁻¹) | ΔH° (kJ mol ⁻¹) | ΔS° (J mol ⁻¹ K ⁻¹) |
|------------|----------------------------------|-------------------------------|-----------|---|---|--|
| 298 | | 1.384 | 0.325 | -0.82 | | |
| 318 | 6.07 | 1.268 | 0.237 | -0.60 | -4.98 | -13.72 |
| 333 | | 1.158 | 0.146 | -0.37 | | |

tive value of entropy (ΔS°) indicated an order at the interface of the adsorbent⁵². Thus, $\Delta H^\circ < 0$ suggested an exothermic process.

The following Arrhenius equation (Eq. 8) allows us to express the activation energy as a function of k_2 and temperature:

$$\ln k_2 = \ln A - \frac{E_a}{RT} \quad (8)$$

where E_a is the activation energy, and A the Arrhenius factor. The values of E_a (Table 4) (6.07 kJ mol^{-1}), and that of enthalpy ($-4.98 \text{ kJ mol}^{-1}$) indicated that the process of CA adsorption by CLDH was governed by a physisorption mechanism⁵³. From these results, it could be argued that CA carboxylate groups are responsible for the interaction with hydroxyl groups of the reconstructed LDH layers⁴⁵.

Adsorption isotherms

Fig. 5 shows the isotherms that express the retained amount of CA as a function of C_e . The study that we conducted was carried out with different initial concentrations of CA (10 mg L^{-1} – 500 mg L^{-1}), and for three different masses of CLDH (10, 30 and 50 mg) for 2 hours of stirring at pH 5.

According to the classification of Giles *et al.*⁵⁴, the isotherms obtained for different masses of CLDH are of type S. This type of isotherm indicates the presence of cooperative adsorption between the adsorbate molecules⁵⁵. The adsorbed CA molecules promote the subsequent adsorption of other molecules. They therefore tend to be adsorbed in groups.

This result shows that the amount of retention of the pollutant is inversely proportional to the mass of the adsorbent material, which allows advancing

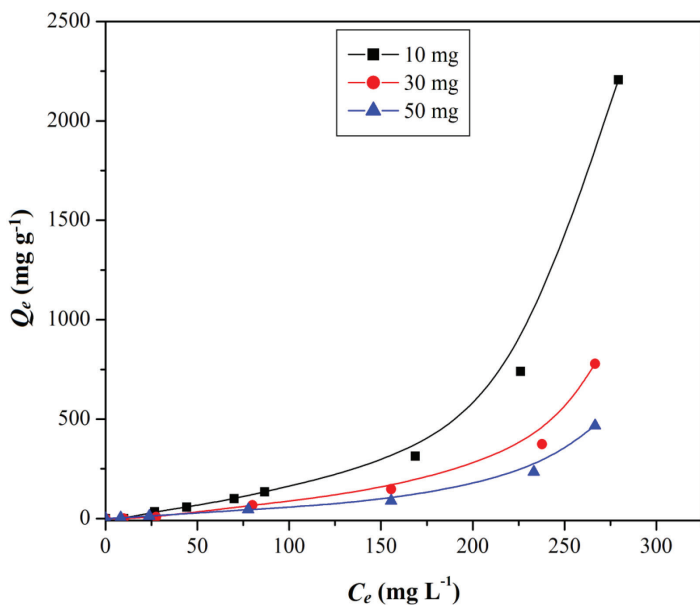


Fig. 5 – Adsorption isotherms of CA determined with three masses of CLDH

Table 4 – Parameter values of Freundlich isotherm model for adsorption of CA by CLDH

| m_{CLDH} (mg) | K_F (mg g^{-1}) | n | R^2 |
|---------------------------|---------------------------------|-------|-------|
| 10 | 0.185 | 0.503 | 0.948 |
| 30 | 0.152 | 0.523 | 0.991 |
| 50 | 0.500 | 0.774 | 0.967 |

and confirming the existence of a cooperative adsorption on the surface and an intercalation of CA between the reconstructed LDH sheets.

The linear transformations of the isotherms gave a good result with the Freundlich model that can be expressed by the following equation⁵⁶:

$$\ln Q_e = \ln K_F + \frac{1}{n} \ln C_e \quad (9)$$

where K_F is the Freundlich constant, and factor n measures the deviation from linearity. The linearisation followed the Freundlich model for three CLDH masses. The parameter values of Freundlich model are presented in Table 4.

From the results presented in Table 4, the value of the heterogeneity factor $1/n$ is greater than 1, which leads to $n < 1$; this result probably implies the existence of a more heterogeneous adsorption surface including the heterogeneous adsorption sites⁵⁷. These results are similar to those obtained in another work⁵⁵. Consequently, the fixing of the CA anions can be explained by electrostatic interactions, on the one hand between the CA molecules, and, on the other hand by hydrogen bonds between the carboxylate groups of CA and the hydroxyl groups of the LDH sheets. In this case, $n < 1$, indicates that the adsorption is normal and cooperative with a convex curve. Thus, we assumed that CA molecules were stacked in multilayer at the reconstructed LDH surface through π - π interactions of the aromatic ring⁴¹.

Effect of mass ratio (CA/CLDH)

To examine the effect of the mass ratio adsorbate/adsorbent on the adsorption capacity of CLDH, the initial concentration of adsorbate CA was varied from 10 mg L^{-1} to 500 mg L^{-1} , with a CLDH mass of 10 mg (Fig. 6) with a pH of 5 for 2 hours.

The optimal mass ratio (CA/CLDH) was 3 with an experimental retention capacity of 2220 mg g^{-1} and a retention rate of 90 %.

The remaining amount of CA in solution was 10 %. This drug was found in wastewater in a range of 1.6 – 5.0 ng L^{-1} ¹⁷, in surface water 0.55 – 103.00 ng L^{-1} ⁵⁸, in groundwater 400 ng L^{-1} ¹⁶, in seawater 0.28 – 1.35 ng L^{-1} , in estuary 18 ng L^{-1} ⁵⁸, and in drinking water the concentration of CA can reach 270 ng L^{-1} ⁵⁹.

The treatment of CA with CLDH can lead to reduced concentrations found in groundwater from 400 ng L⁻¹ to 40 ng L⁻¹, and for tap water to 27 ng L⁻¹. By comparing the remaining amount of CA with the results of the other works mentioning its presence in different media, it can be pointed out that this is much lower than the tolerance threshold of 170 ng L⁻¹ 60.

Study by X-ray diffraction

The diffractogram obtained after retention (Fig. 7) indicated the reconstruction of two phases, one intercalated by CA, and the other due to slight contamination by carbonate anions. The latter kept the same interlamellar distance as the starting matrix before calcination (0.764 nm).

For the first phase, there was a shift in the line (003) towards the low values at 2θ indicating the intercalation of the CA anion between the recon-

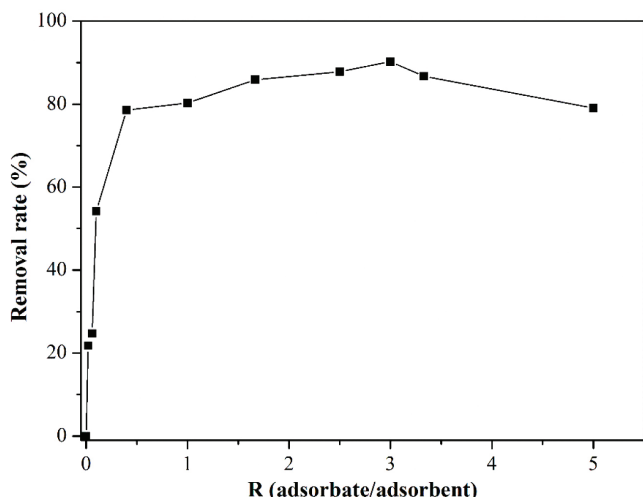


Fig. 6 – CA removal rate as a function of the mass ratio (CA/CLDH)

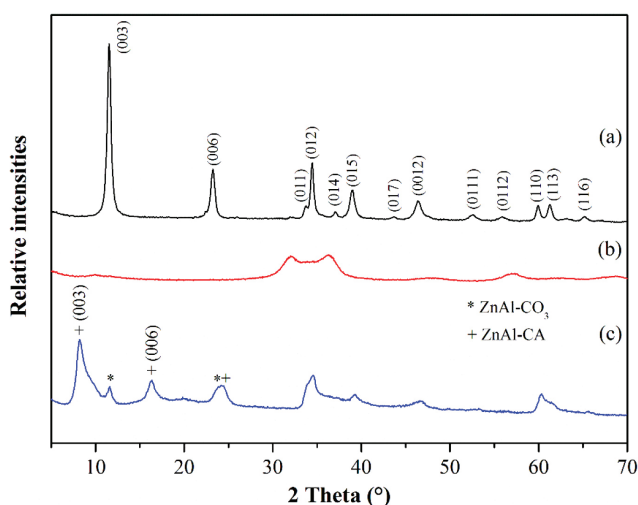


Fig. 7 – Powder XRD patterns of LDH (a), CLDH (b), and ZnAl-CA phase obtained after retention of CA (c) (m_{CLDH} = 30 mg, [CA] = 500 mg L⁻¹, pH = 5, tc = 2 h)

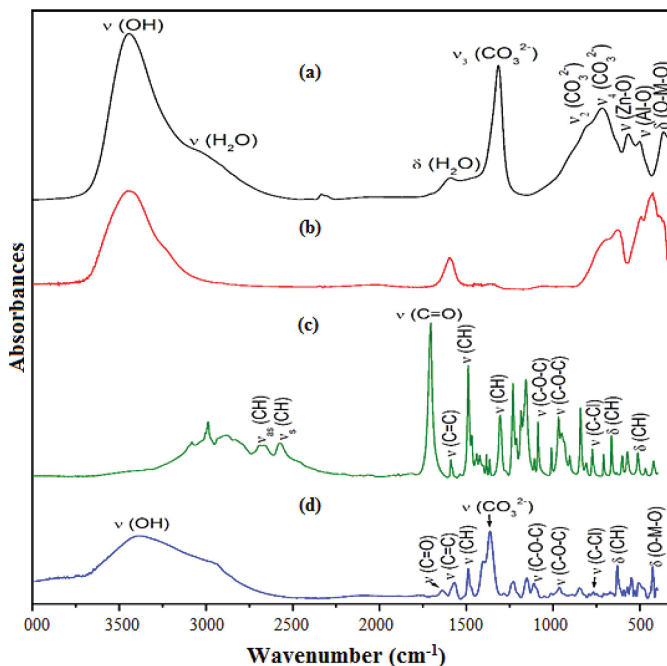


Fig. 8 – IR spectra of LDH (a), CLDH (b), CA (c), and the obtained phase ZnAl-CA after retention of CA (d) (m_{CLDH} = 30 mg, [CA] = 500 mg L⁻¹, pH = 5, tc = 2 h)

structed LDH sheets with an interlamellar distance equal to 1.07 nm. The appearance of the lines around 61° in 2θ specific to (110) and (113) confirmed the reconstruction of an LDH phase (hydroxalcite type) 61.

The lattice parameters for this phase intercalated by CA ZnAl-CA were: a = 0.306 nm, c = 3.21 nm, and the interlamellar distance d = 1.07 nm.

Study by infrared spectroscopy

The IR spectra were made to obtain information concerning the vibrations of the functional groups of the material and the pharmaceutical product CA before and after retention. Fig. 8 shows the characteristic bands of CLDH, CA, and LDH phases before and after the retention process. With regard to the phase obtained after retention, we observed the appearance of metal-oxygen vibration bands for Zn-O around 615 cm⁻¹, and for Al-O around 554 cm⁻¹. The appearance of a band around 3430 cm⁻¹ corresponded to the valence vibrations of OH, the vibration bands ν_s(CH) and ν_{as}(CH) were at 2600 and 2700 cm⁻¹, respectively, and a characteristic vibration band of the group (C = O) was at 1702 cm⁻¹. The bands between 1000 and 1400 cm⁻¹, were characteristic of the mode (C-O-C), the benzene ring (C=C) bands were around 840 cm⁻¹, and the vibration band ν(C-Cl) around 774 cm⁻¹ 41,62. On the other hand, the bands at 400 cm⁻¹ were characteristic of LDH sheets reconstructed from the rehydration of mixed oxides 30. These IR spectroscopy results confirmed that the adsorbent material had retained the drug CA by the appearance of its characteristic bands.

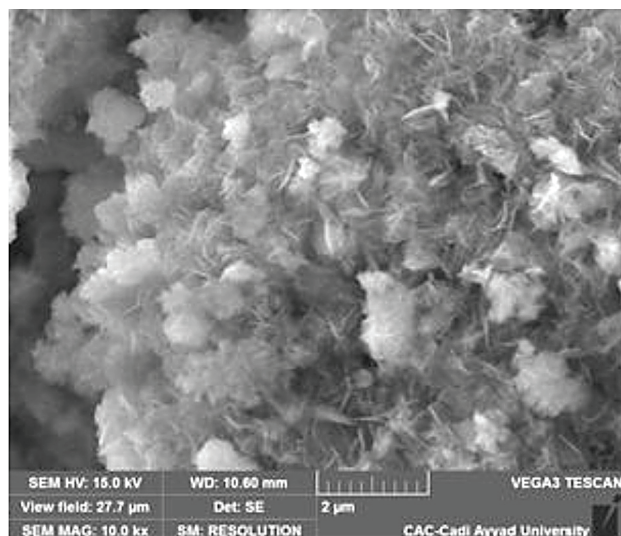


Fig. 9 – SEM photograph of the obtained phase ZnAl-CA after retention ($m_{\text{CLDH}} = 30 \text{ mg}$, $[\text{CA}] = 500 \text{ mg L}^{-1}$, $\text{pH} = 5$, $t_c = 2 \text{ h}$)

Analysis by scanning electron microscopy

The SEM photograph (Fig. 9) corresponds to the phase obtained after retention of CA. The sample studied shows aggregates including crystallites with different sizes. This result confirmed that, after retention of CA by CLDH, we had witnessed the appearance of lamellar character, proving the reconstruction of an LDH phase from mixed oxides by means of their conserved memory effect.

Thermogravimetric analysis

The results of thermogravimetric analysis specific to the free pharmaceutical product CA and to the phase ZnAl-CA obtained after its retention by CLDH are shown in Fig. 10.

For free product CA (Fig. 10a), a first loss was observed, which started from 25 °C to 170 °C (2.5 %), corresponding to the elimination of adsorbed water by the product, followed by three successive losses (DTG) ending around 550 °C, which were due to the total decomposition of the organic matter.

In the case of intercalation of this pharmaceutical compound between the LDH sheets (Fig. 10b), it was observed that the loss of mass took place in four stages:

- Between 25 °C and 90 °C, a loss of 3 % of mass due to the water adsorbed physically by the material.

- A loss of 10 %, between 100 °C and 220 °C, due to the removal of the intercalated water.

- Between 220 °C and 450 °C, a loss of 9 % was observed, which corresponded to the dehydroxylation and decomposition of carbonate anions^{41,63}.

We should point out a slight delay in decomposition of the same matter compared to the ZnAl-CO₃ phase (Fig. 1b), which may be due to the intercalation of CA anions interacting with the hydroxyl groups of the reconstructed LDH sheets.

- The last loss that ended above 800 °C (> 8 %) was due to the decomposition of organic matter; this delay was probably due to the role that LDH can play as stabilizer of organic matter decomposition. LDH had relatively improved the stability of decomposition after thermal treatment of the pharmaceutical compound. Consequently, the LDH-drug hybrid compound supported the safe preservation of this type of drug⁴¹.

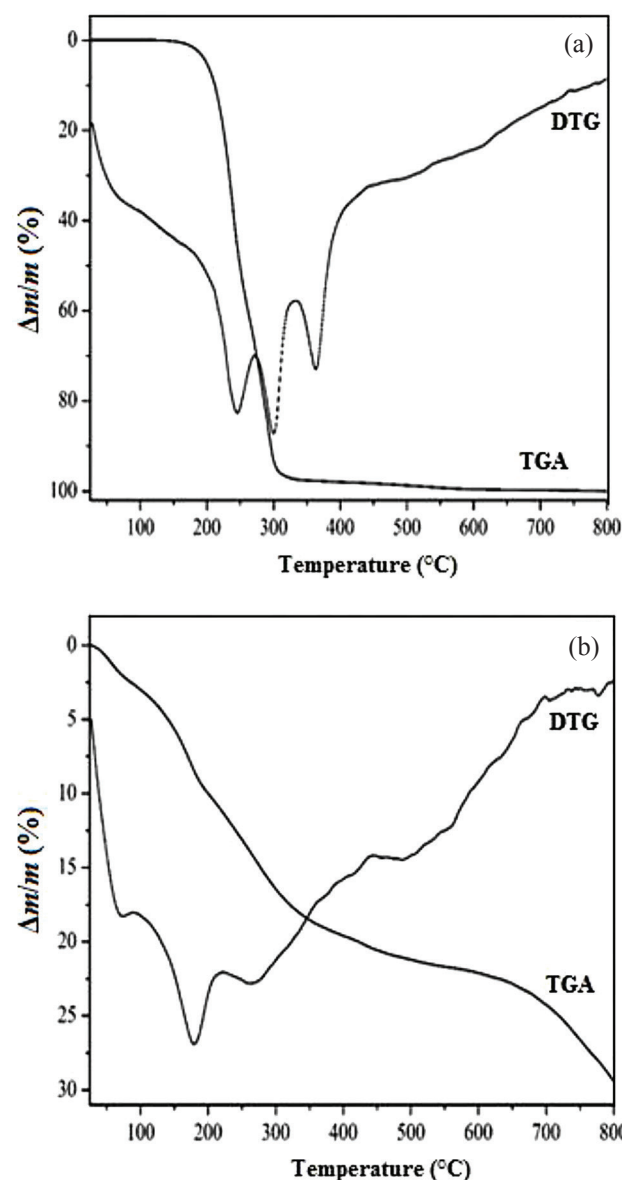


Fig. 10 – Analysis TGA/DTG of free drug CA (a), and after its retention by CLDH (b) ($m_{\text{CLDH}} = 30 \text{ mg}$, $[\text{CA}] = 500 \text{ mg L}^{-1}$, $\text{pH} = 5$, $t_c = 2 \text{ h}$)

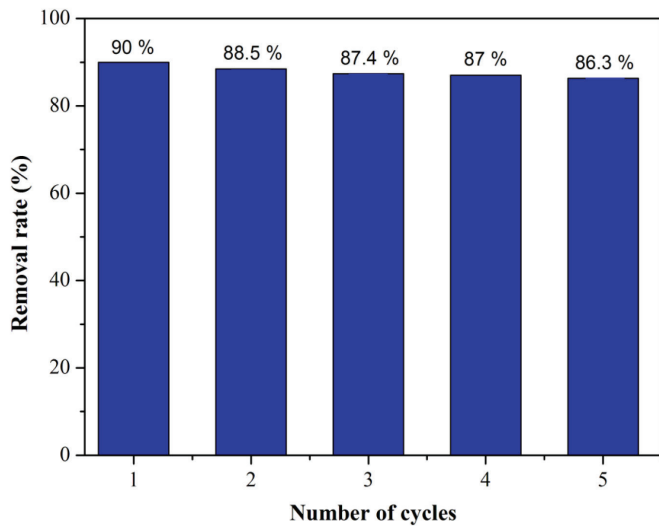


Fig. 11 – Recycling efficiency of CLDH after retention of CA for a CA/CLDH mass ratio of 3

Recycling and regeneration of the adsorbent material

The removal rate of CA by CLDH depends on the percentage of CA remaining after repeated cycles, while using the optimal mass ratio CA/CLDH of 3, which corresponds to a maximum removal rate of CA of 90 %. Each cycle firstly comprised the retention of CA under optimal conditions; secondly, an anionic exchange reaction with a solution of

Na_2CO_3 (1 mol L^{-1}) in order to replace all the intercalated and adsorbed CA anions after reconstruction of the LDH phase, because the carbonates have a very high affinity for LDH sheets³⁷, and finally, calcination at $500 \text{ }^\circ\text{C}$ of the new carbonated LDH phase. The elimination rate of CA was calculated by the following equation:

$$\% \text{ Removal rate} = \frac{(C_i - C_e) \cdot 100}{C_i} \quad (10)$$

where, C_i and C_e are the initial and equilibrium concentrations of CA, respectively.

The removal rate of CA decreased from 90 % to 86.3 % after five recycling cycles (Fig. 11). This led us to consider that the used LDH material was an efficient adsorbent for CA elimination and it was perfectly recyclable. However, the residual quantities of the pollutant in solution are much lower than the tolerated thresholds⁶⁰. The reuse of the material, previously discharged by anionic exchange reaction, was carried out under optimal experimental conditions in the adsorption cycles.

Structural model

To determine the orientation of the intercalated CA, we calculated the length of the molecule using the software Gaussian 03. The calculated values of the three possible orientations of CA are presented in Fig. 12. The proposed orientation (A) seems the

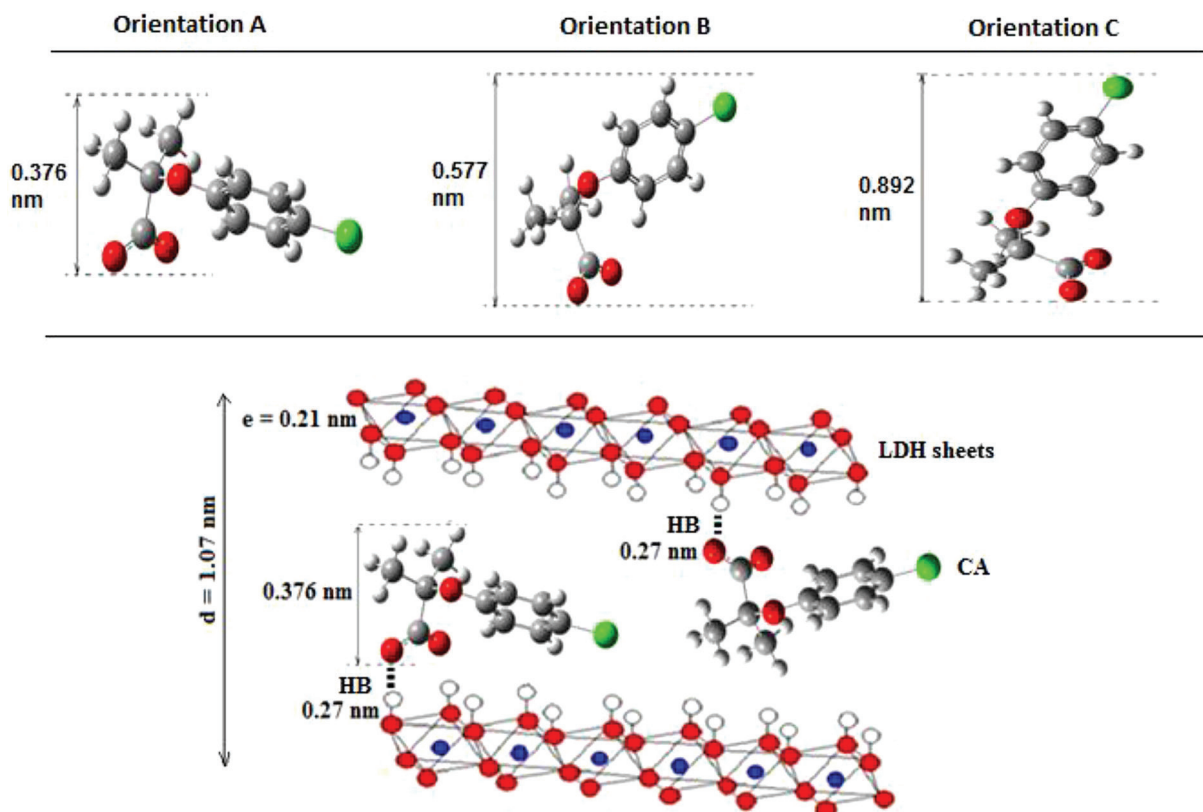


Fig. 12 – Structural model of CA orientation between LDH sheets

Table 5 – Maximum adsorption capacity and removal rate of CA on different materials

| Adsorbents | Q_m (mg g ⁻¹) | Removal rate (%) | pH | References |
|--|--------------------------------|---------------------|---------|------------|
| Porous coal derived from Bio-MOF-1 | 540 | - | 7 | 65 |
| Charcoal developed from cotton fabric residues | 80 | 83 | 7.5 | 36 |
| Activated carbon | 211.9 | 70 | 3 and 8 | 64 |
| Chitosan modified with polyethyleneimine | 349 | 82.7 | 4 | 34 |
| Calcined inorganic-organic clays (CoAlO _r -NaBt, CuAlO _r -NaBt, NiAlO _r -NaBt) | 5.48 | - | 12 | 66 |
| Rice straw for agricultural waste | 126.3 | 42.5 | 4 | 45 |
| Activated carbon made from cork | 139-295 | 5 | 2 | 67 |
| Bentonite modified with Ni-Al-HDTMA | 0.64 | - | 2.97 | 68 |
| Mesoporous silica SBA-15 | 0.07 | 49 | 3 | 69 |
| Granulated cork | 0.06 | 21 | 7 | 70 |
| Clay aggregates (LECA) | 0.027 | 51.4 | 6.29 | 13 |
| Plant <i>Typha</i> spp | - | 80 | 6 | 33 |
| Calcined anionic clay ZnAl-CO ₃ | 2220 | 90 | 5 | This work |

most likely of the pollutant CA intercalated between the LDH sheets.

The interlamellar distance determined experimentally was 1.07 nm, and required that the COO⁻ groups of CA could be oriented towards the LDH sheets, suggesting a horizontal disposition of the CA anion. This arrangement resulted in an interlamellar dimension of CA of 0.376 nm. Knowing the thickness of the LDH sheet, which is equal to 0.21 nm, and the length of the hydrogen bond, which is of the order of 0.27 nm, we obtain:

$$d = 0.27 + 0.21 + 0.376 = 0.856 \text{ nm} < 1.07 \text{ nm}$$

It can be seen that the distance found theoretically is lower than that found experimentally by 0.21 nm. This difference may probably be due to the existence of repulsive interactions between hydrogen atoms of LDH sheets and those of CA. In another work concerning the retention of CA by LDH based on Mg-Al, the authors found a vertical arrangement of CA between LDH sheets with an interlayer distance of 2.11 nm⁴¹.

Comparative study

In Table 5, shows some results concerning the retention of CA by different adsorbents, such as cationic or anionic clays, activated carbon, metal-organic composites, and mesoporous silica. However, the adsorption capacity of activated carbon⁶⁴ and metal-organic composites is not very high, and the mesoporous silica has a slow adsorption rate with a low adsorption capacity.

The comparison of these results suggests that the CLDH adsorbent used in this work has a very interesting efficiency compared to other materials. The quantity retained is much higher, as is the rate of elimination. In addition, this material is recyclable by anionic exchange with carbonates, which will also allow us to recover pollutants.

Conclusion

The calcined anionic clay ZnAl-CO₃ used in this study has shown its high retention capacity of the highly persistent drug CA present in drinking water, groundwater, surface water, and seawater. The optimal removal was performed at pH 5, the retention kinetics were fast and followed the pseudo-second order model, while the isotherms were governed by Freundlich model (multilayer adsorption), and they were of S type, implying a cooperative adsorption. The retention capacity exceeded 2220 mg g⁻¹ for an optimum mass ratio (CA/CLDH) of 3. The removal rate reached 90 %, and the remaining amount was well below the tolerance thresholds. From the thermodynamic study, a physical process governed the retention process. The techniques used confirmed the retention of CA by adsorption on the surface of LDH phase and by intercalation. The comparative study showed that this material is promising and very effective compared to other adsorbents for the elimination of this pollutant.

References

1. *Fatta-Kassinos, D., Meric, S., Nikolaou, A.*, Pharmaceutical residues in environmental waters and wastewater: Current state of knowledge and future research, *Anal. Bioanal. Chem.* **399** (2011) 251.
doi: <https://doi.org/10.1007/s00216-010-4300-9>
2. *Kümmerer, K.*, The presence of pharmaceuticals in the environment due to human use – present knowledge and future challenges, *J. Environ. Manage.* **90** (2009) 2354.
doi: <https://doi.org/10.1016/j.jenvman.2009.01.023>
3. *Boyd, G. R., Reemtsma, H., Grimm, D. A., Mitra, S.*, Pharmaceuticals and personal care products (PPCPs) in surface and treated waters of Louisiana, USA and Ontario, Canada, *Sci. Total Environ.* **311** (2003) 135.
doi: [https://doi.org/10.1016/S0048-9697\(03\)00138-4](https://doi.org/10.1016/S0048-9697(03)00138-4)
4. *Tixier, C., Singer, H. P., Oellers, S., Müller, S. R.*, Occurrence and fate of carbamazepine, clofibrac acid, diclofenac, ibuprofen, ketoprofen, and naproxen in surface waters, *Environ. Sci. Technol.* **37** (2003) 1061.
doi: <https://doi.org/10.1021/es025834r>
5. *Xu, W., Zhang, G., Li, X., Zou, S., Li, P., Hu, Z., Li, J.*, Occurrence and elimination of antibiotics at four sewage treatment plants in the Pearl River Delta (PRD), South China, *Water Res.* **41** (2007) 4526.
doi: <https://doi.org/10.1016/j.watres.2007.06.023>
6. *Kasprzyk-Hordern, B., Dinsdale, R. M., Guwy, A. J.*, The occurrence of pharmaceuticals, personal care products, endocrine disruptors and illicit drugs in surface water in South Wales, UK, *Water Res.* **42** (2008) 3498.
doi: <https://doi.org/10.1016/j.watres.2008.04.026>
7. *Jones, O. A., Voulvoulis, N., Lester, J. N.*, The occurrence and removal of selected pharmaceutical compounds in a sewage treatment works utilising activated sludge treatment, *Environ. Pollut.* **145** (2007) 738.
doi: <https://doi.org/10.1016/j.envpol.2005.08.077>
8. *Weigel, S., Kuhlmann, J., Hühnerfuss, H.*, Drugs and personal care products as ubiquitous pollutants: Occurrence and distribution of Clofibrac acid, caffeine and DEET in the North Sea, *Sci. Total Environ.* **295** (2002) 131.
doi: [https://doi.org/10.1016/S0048-9697\(02\)00064-5](https://doi.org/10.1016/S0048-9697(02)00064-5)
9. *Thomas, K. V., Hilton, M. J.*, The occurrence of selected human pharmaceutical compounds in UK estuaries, *Mar. Pollut. Bull.* **49** (2004) 436.
doi: <https://doi.org/10.1016/j.marpolbul.2004.02.028>
10. *Focazio, M. J., Kolpin, D. W., Barnes, K. K., Furlong, E. T., Meyer, M. T., Zaugg, S. D., Barber, L. B., Thurman, M. E.*, A national reconnaissance for pharmaceuticals and other organic wastewater contaminants in the United States – II) Untreated drinking water sources, *Sci. Total Environ.* **402** (2008) 201.
doi: <https://doi.org/10.1016/j.scitotenv.2008.02.021>
11. *Gagné, F., Blaise, C., André, C.*, Occurrence of pharmaceutical products in a municipal effluent and toxicity to rainbow trout (*Oncorhynchus mykiss*) hepatocytes, *Ecotoxicol. Environ. Saf.* **64** (2006) 329.
doi: <https://doi.org/10.1016/j.ecoenv.2005.04.004>
12. *Nassef, M., Matsumoto, S., Seki, M., Khalil, F., Kang, I. J., Shimasaki, Y., Oshima, Y., Honjo, T.*, Acute effects of triclosan, diclofenac and carbamazepine on feeding performance of Japanese medaka fish (*Oryzias latipes*), *Chemosphere* **80** (2010) 1095.
doi: <https://doi.org/10.1016/j.chemosphere.2010.04.073>
13. *Dordio, A. V., Estêvão Candeias, A. J., Pinto A. P., da Costa, C. T., Carvalho, A. J. P.*, Preliminary media screening for application in the removal of clofibrac acid, carbamazepine and ibuprofen by SSF-constructed wetlands, *Ecol. Eng.* **35** (2009a) 290.
doi: <https://doi.org/10.1016/j.ecoleng.2008.02.014>
14. *Salgado, R., Oehmen, A., Carvalho, G., Noronha, J. P., Reis, M. A. M.*, Biodegradation of clofibrac acid and identification of its metabolites, *J. Hazard. Mater.* **241–242** (2012) 182.
doi: <https://doi.org/10.1016/j.jhazmat.2012.09.029>
15. *Khetan, S. K., Collins, T. J.*, Human pharmaceuticals in the aquatic environment: A challenge to green chemistry, *Chem. Rev.* **107** (2007) 2319.
doi: <https://doi.org/10.1021/cr020441w>
16. *Heberer, T.*, Occurrence, fate, and removal of pharmaceutical residues in the aquatic environment: A review of recent research data, *Toxicol. Lett.* **131** (2002) 5.
doi: [https://doi.org/10.1016/S0378-4274\(02\)00041-3](https://doi.org/10.1016/S0378-4274(02)00041-3)
17. *Ternes, T. A.*, Occurrence of drugs in German sewage treatment plants and rivers, *Water Res.* **32** (1998) 3245.
doi: [https://doi.org/10.1016/S0043-1354\(98\)00099-2](https://doi.org/10.1016/S0043-1354(98)00099-2)
18. *Matamoros, V., Garcia, J., Bayona, J. M.*, Organic micropollutant removal in a full-scale surface flow constructed wetland fed with secondary effluent, *Water Res.* **42** (2008) 653.
doi: <https://doi.org/10.1016/j.watres.2007.08.016>
19. *Iqbal, J., Shah, N. S., Sayed, M., Muhammad, N., Rehman, S., Ali Khan, J., Khan, Z., Howari, F. M., Nazzal, Y., Xavier, C., Arshad, S., Hussein, A., Polychronopoulou, K.*, Deep eutectic solvent-mediated synthesis of ceria nanoparticles with the enhanced yield for photocatalytic degradation of flumequine under UV-C, *J. Water Process Eng.* **33** (2020) 101012.
doi: <https://doi.org/10.1016/j.jwpe.2019.101012>
20. *Zhou, Z., Ma, J., Liu, X., Lin, C., Sun, K., Zhang, H., Li, X., Fan, G.*, Activation of peroxydisulfate by nanoscale zero-valent iron for sulfamethoxazole removal in agricultural soil: Effect, mechanism and ecotoxicity, *Chemosphere* **223** (2019) 196.
doi: <https://doi.org/10.1016/j.chemosphere.2019.02.074>
21. *Briche, S., Derqaoui, M., Belaiche, M., El Mouchtari, E., Wong-Wah-Chung, P., Rafiqah, S.*, Nanocomposite material from TiO₂ and activated carbon for the removal of pharmaceutical product sulfamethazine by combined adsorption/photocatalysis in aqueous media, *Environ. Sci. Pollut. Res. Int.* (2020).
doi: <https://doi.org/10.1007/s11356-020-08939-2>
22. *Al-Maqdi, K. A., Hisaindee, S., Rauf, M. A., Ashraf, A. A.*, Detoxification and degradation of sulfamethoxazole by soybean peroxidase and UV + H₂O₂ remediation approaches, *Chem. Eng. J.* **352** (2018) 450.
doi: <https://doi.org/10.1016/j.cej.2018.07.036>
23. *Cai, H., Zhao, T., Ma, Z., Liu, J.*, Efficient removal of metronidazole by the photo-Fenton process with a magnetic Fe₃O₄@PBC composite, *J. Environ. Eng.* **146** (2020) 04020056.
doi: [https://doi.org/10.1061/\(ASCE\)EE.1943-7870.0001735](https://doi.org/10.1061/(ASCE)EE.1943-7870.0001735)
24. *Ducey, T. F., Collins, J. C., Ro, K. S., Woodbury, B. L., Griffin, D. D.*, Hydrothermal carbonization of livestock mortality for the reduction of pathogens and microbially-derived DNA, *Front. Environ. Sci. Eng.* **11** (2017) 9.
doi: <https://doi.org/10.1007/s11783-017-0930-x>
25. *Maged, A., Iqbal, J., Kharbish, S., Ismael, I. S., Bhatnagar, A.*, Tuning tetracycline removal from aqueous solution onto activated 2:1 layered clay mineral: Characterization, sorption and mechanistic studies, *J. Hazard. Mater.* **384** (2020) 121320.
doi: <https://doi.org/10.1016/j.jhazmat.2019.121320>

26. Alatalo, S. M., Daneshvar, E., Kinnunen, N., Meščeriakovas, A., Thangaraj, S. K., Jänis, J., Tsang, D. C. W., Bhatnagar, A., Lähde, A., Mechanistic insight into efficient removal of tetracycline from water by Fe/grapheme, *Chem. Eng. J.* **373** (2019) 821.
doi: <https://doi.org/10.1016/j.cej.2019.05.118>
27. Balasubramani, K., Sivarajasekar, N., Naushad, M., Effective adsorption of antidiabetic pharmaceutical (metformin) from aqueous medium using graphene oxide nanoparticles: Equilibrium and statistical modeling, *J. Mol. Liq.* **301** (2020) 112426.
doi: <https://doi.org/10.1016/j.molliq.2019.112426>
28. Banu Yener, H., Removal of cefdinir from aqueous solution using nanostructure adsorbents of TiO₂, SiO₂ and TiO₂/SiO₂: Equilibrium, thermodynamic and kinetic studies, *Chem. Biochem. Eng. Q.* **33** (2019) 235.
doi: <https://doi.org/10.15255/CABEQ.2019.1632>
29. Vrbková, E., Výsokčilová, E., Semrádová, A., Sekerová, L., Červený, L., Mixed oxides as successful sorption materials for some active pharmaceutical ingredients, *Chem. Biochem. Eng. Q.* **34** (2020) 25.
doi: <https://doi.org/10.15255/CABEQ.2020.1774>
30. Mourid, E., Lakraimi, M., El Abridi, S., Benaziz, L., Elkhatibi, E., Berraho, M., Use of calcined layered double hydroxide [Zn₂-Al-CO₃] for removal of textile dye acid green 1 from wastewater: kinetic, equilibrium, comparative, and recycling studies, *Turkish J. Chem.* **42** (2018) 1146.
doi: <https://doi.org/10.3906/kim-1705-48>
31. Gholami, P., Khataee, A., Soltani, R. D. C., Dinpazhoh, L., Bhatnagar, A., Photocatalytic degradation of gemifloxacin antibiotic using Zn-Co-LDH@biochar nanocomposite, *J. Hazard. Mater.* **382** (2020) 121070.
doi: <https://doi.org/10.1016/j.jhazmat.2019.121070>
32. Mourid, E., El Mouchtari, E., El Mersly, L., Benaziz, L., Rafiqah, S., Lakraimi, M., Development of a new recyclable nanocomposite LDH-TiO₂ for the degradation of antibiotic sulfamethoxazole under UVA radiation: An approach towards sunlight, *J. Photochem. Photobiol. A: Chem.* **396** (2020) 112530.
doi: <https://doi.org/10.1016/j.jphotochem.2020.112530>
33. Dordio, A. V., Duarte, C., Barreiros, M., Carvalho, A. J. P., Pinto, A. P., da Costa, C. T., Toxicity and removal efficiency of pharmaceutical metabolite clofibrac acid by *Typha* spp – Potential use for phytoremediation, *Bioresour. Technol.* **100** (2009b) 1156.
doi: <https://doi.org/10.1016/j.biortech.2008.08.034>
34. Nie, Y., Deng, S., Wang, B., Huang, J., Yu, G., Removal of clofibrac acid from aqueous solution by polyethylenimine-modified chitosan beads, *Front. Environ. Sci. Eng.* **8** (2014) 675.
doi: <https://doi.org/10.1007/s11783-013-0622-0>
35. Lu, X., Shao, Y., Gao, N., Chen, J., Zhang, Y., Wang, Q., Lu, Y., Adsorption and removal of clofibrac acid and diclofenac from water with MIEX resin, *Chemosphere* **161** (2016) 400.
doi: <https://doi.org/10.1016/j.chemosphere.2016.07.025>
36. Boudrahem, N., Delpeux-Ouldriane, S., Khenniche, L., Boudrahem, F., Aissani-Benissad, F., Gineys, M., Single and mixture adsorption of clofibrac acid, tetracycline and paracetamol onto activated carbon developed from cotton cloth residue, *Process Saf. Environ. Prot.* **111** (2017) 544.
doi: <https://doi.org/10.1016/j.psep.2017.08.025>
37. Iyi, N., Matsumoto, T., Kaneko, Y., Kitamura, K., Deintercalation of carbonate ions from a hydrotalcite-like compound: Enhanced decarbonation using acid-salt mixed solution, *Chem. Mater.* **16** (2004) 2926.
doi: <https://doi.org/10.1021/cm049579g>
38. Biswas, A. K., Sahoo, J., Chatli, M. K., A Simple UV-Vis spectrophotometric method for determination of beta-carotene content in raw carrot, sweet potato and supplemented chicken meat nuggets, *Lwt-Food Sci. Technol.* **44** (2011) 1809.
doi: <https://doi.org/10.1016/j.lwt.2011.03.017>
39. Kameda, T., Saito, M., Umetsu, Y., Preparation and characterisation of Mg–Al layered double hydroxides intercalated with 2-naphthalene sulphonate and 2,6-naphthalene disulphonate, *Mater. Trans.* **47** (2006) 923.
doi: <https://doi.org/10.2320/matertrans.47.923>
40. Legrouri, A., Lakraimi, M., Barroug, A., De Roy, A., Besse, J. P., Removal of the herbicide 2,4-dichlorophenoxyacetate from water to zinc–aluminium–chloride layered double hydroxides, *Water Res.* **39** (2005) 3441.
doi: <https://doi.org/10.1016/j.watres.2005.03.036>
41. Berber, M. R., Hafez, I. H., Minagawa, K., Mori, T., Tanaka, M., Nanocomposite formulation system of lipid-regulating drugs based on layered double hydroxide: Synthesis, characterization and drug release properties, *Pharm. Res.* **27** (2010) 2394.
doi: <https://doi.org/10.1007/s11095-010-0175-x>
42. Alvarez, R., Toffolo, A., Pérez, V., Linares, C. F., Synthesis and characterization of CoMo/Zn–Al mixed oxide catalysts for hydrodesulphuration of thiophene, *Catal Lett.* **137** (2010) 150.
doi: <https://doi.org/10.1007/s10562-010-0337-9>
43. Gastuche, M. C., Brown, G., Mortland, M. M., Mixed magnesium aluminium hydroxides. I. Preparation and characterization of compounds formed in dialysed systems, *Clay Miner.* **7** (1967) 177.
doi: <https://doi.org/10.1180/claymin.1967.007.2.05>
44. Pradeep, A., Priyadharsini, P., Chandrasekaran, G., Sol-gel route of synthesis of nanoparticles of MgFe₂O₄ and XRD, FTIR and VSM study, *J. Magn. Magn. Mater.* **320** (2008) 2774.
doi: <https://doi.org/10.1016/j.jmmm.2008.06.012>
45. Liu, Z., Zhou, X., Chen, X., Dai, C., Zhang, J., Zhang, Y., Biosorption of clofibrac acid and carbamazepine in aqueous solution by agricultural waste rice straw, *J. Environ. Sci.* **25** (2013) 2384.
doi: [https://doi.org/10.1016/S1001-0742\(12\)60324-6](https://doi.org/10.1016/S1001-0742(12)60324-6)
46. Cheung, W. H., Szeto, Y. S., McKay, G., Intraparticle diffusion processes during acid dye adsorption onto chitosan, *Bioresour. Technol.* **98** (2007) 2897.
doi: <https://doi.org/10.1016/j.biortech.2006.09.045>
47. Idan, I. J., Abdullah, L. C., Choong, T. S. Y., Jamil, S. N., Equilibrium, kinetics and thermodynamic adsorption studies of acid dyes on adsorbent developed from kenaf core fiber, *Adsorpt. Sci. Technol.* **36** (2018) 694.
doi: <https://doi.org/10.1177/0263617417715532>
48. Dotto, G. L., Buriol, C., Pinto, L. A. A., Diffusional mass transfer model for the adsorption of food dyes on chitosan films, *Chem. Eng. Res. Des.* **92** (2014) 2324.
doi: <https://doi.org/10.1016/j.cherd.2014.03.013>
49. Li, D., Yan, J., Liu, Z., Liu, Z., Adsorption kinetic studies for removal of methylene blue using activated carbon prepared from sugar beet pulp, *Int. J. Environ. Sci. Technol.* **13** (2016) 1815.
doi: <https://doi.org/10.1007/s13762-016-1012-5>
50. Kannan, N., Sundaram, M. M., Kinetics and mechanism of removal of methylene blue by adsorption on various carbons — a comparative study, *Dyes Pigm.* **51** (2001) 25.
doi: [https://doi.org/10.1016/S0143-7208\(01\)00056-0](https://doi.org/10.1016/S0143-7208(01)00056-0)

51. Kyzas, G. Z., Travlou, N. A., Kalogirou, O., Deliyanni, E. A., Magnetic graphene oxide: Effect of preparation route on reactive black 5 adsorption, *Materials* **6** (2013) 1360. doi: <https://doi.org/10.3390/ma6041360>
52. Sari, A., Tuzen, M., Citak, D., Soylak, M., Equilibrium, kinetic and thermodynamic studies of adsorption of Pb(II) from aqueous solution onto Turkish kaolinite clay, *J. Hazard. Mater.* **149** (2007) 283. doi: <https://doi.org/10.1016/j.jhazmat.2007.03.078>
53. Zhao, D., Sheng, G., Hu, J., Chen, C., Wang, X., The adsorption of Pb(II) on Mg₃Al layered double hydroxide, *Chem. Eng. J.* **171** (2011) 167. doi: <https://doi.org/10.1016/j.cej.2011.03.082>
54. Giles, C. H., MacEwan, T. H., Nakhwa, S. N., Smith, D., Studies in adsorption. Part XI. A System of classification of solution adsorption isotherms and its use in diagnosis of adsorption mechanisms and in measurement of specific surface areas of solids, *J. Chem. Soc.* **14** (1960) 3973. doi: <https://doi.org/10.1039/JR9600003973>
55. Giles, C. H., D'Silva, A. P., Easton, I. A., A general treatment and classification of the solute adsorption isotherm. II. Experimental interpretation, *J. Colloid Interface Sci.* **47** (1974) 766. doi: [https://doi.org/10.1016/0021-9797\(74\)90253-7](https://doi.org/10.1016/0021-9797(74)90253-7)
56. Yuan, X., Wang, Y., Wang, J., Zhou, C., Tang, Q., Rao, X., Calcined Graphene/MgAl-layered double hydroxides for enhanced Cr(VI) removal, *Chem. Eng. J.* **221** (2013) 204. doi: <https://doi.org/10.1016/j.cej.2013.01.090>
57. Sevim, A. M., Hojiyev, R., Gül, A., Çelik, M. S., An investigation of the kinetics and thermodynamics of the adsorption of a cationic cobalt porphyrine onto sepiolite, *Dyes Pigm.* **88** (2011) 25. doi: <https://doi.org/10.1016/j.dyepig.2010.04.011>
58. Nunes, B., Gaio, A. R., Carvalho, F., Guilhermino, L., Behaviour and biomarkers of oxidative stress in *Gambusia holbrooki* after acute exposure to widely used pharmaceuticals and a detergent, *Ecotoxicol. Environ. Saf.* **71** (2008) 341. doi: <https://doi.org/10.1016/j.ecoenv.2007.12.006>
59. Heberer, T., Stan, H. J., Determination of clofibrilic acid and N-(phenylsulfonyl)-sarcosine in sewage, river and drinking water, *Int. J. Environ. Anal. Chem.* **67** (1997) 113. doi: <https://doi.org/10.1080/03067319708031398>
60. Tauxe-Wuersch, A., De Alencastro, L. F., Grandjean, D., Tarradellas, J., Occurrence of several acidic drugs in sewage treatment plants in Switzerland and risk assessment, *Water Res.* **39** (2005) 1761. doi: <https://doi.org/10.1016/j.watres.2005.03.003>
61. Ni, Z. M., Xia, S. J., Wang, L. G., Xing, F. F., Pan, G. X., Treatment of methyl orange by calcined layered double hydroxides in aqueous solution: Adsorption property and kinetic studies, *J. Colloid Interface Sci.* **316** (2007) 284. doi: <https://doi.org/10.1016/j.jcis.2007.07.045>
62. Hamada, Y. Z., Badr, M. Z., Darboe, H. A., Copper-hydroxo chelates of clofibrilic acid (CA): Reaction of Cu²⁺ with CA, *J. Heavy Met. Toxicity Dis.* **1** (2016) 1. doi: <https://doi.org/10.21767/2473-6457.100013>
63. Lopez, T., Bosch, P., Asomoza, M., Gomez, R., Ramos, E., DTA-TGA and FTIR spectroscopies of sol-gel hydrotalcites: Aluminum source effect on physicochemical properties, *Mater. Lett.* **31** (1997) 311. doi: [https://doi.org/10.1016/S0167-577X\(96\)00296-0](https://doi.org/10.1016/S0167-577X(96)00296-0)
64. Mestre, A. S., Nabiço, A., Figueiredo, P. L., Pinto, M. L., Santos, M. S. C. S., Fonseca, I. M., Enhanced clofibrilic acid removal by activated carbons: Water hardness as a key parameter, *Chem. Eng. J.* **286** (2016) 538. doi: <https://doi.org/10.1016/j.cej.2015.10.066>
65. Bhadra, B. N., Jhung, S. H., Adsorptive removal of wide range of pharmaceuticals and personal care products from water using bio-MOF-1 derived porous carbon, *Microporous Mesoporous Mater.* **270** (2018) 102. doi: <https://doi.org/10.1016/j.micromeso.2018.05.005>
66. Cabrera-Lafaurie, W. A., Román, F. R., Hernández-Maldonado, A. J., Transition metal modified and partially calcined inorganic – organic pillared clays for the adsorption of salicylic acid, clofibrilic acid, carbamazepine, and caffeine from water, *J. Colloid Interface Sci.* **386** (2012) 381. doi: <https://doi.org/10.1016/j.jcis.2012.07.037>
67. Mestre, A. S., Pinto, M. L., Pires, J., Nogueira, J. M. F., Carvalho, A. P., Effect of solution pH on the removal of clofibrilic acid by cork-based activated carbons, *Carbon* **48** (2010) 972. doi: <https://doi.org/10.1016/j.carbon.2009.11.013>
68. Rivera-Jimenez, S. M., Lehner, M. M., Cabrera-Lafaurie, W. A., Hernández-Maldonado, A. J., Removal of naproxen, salicylic acid, clofibrilic acid, and carbamazepine by water phase adsorption onto inorganic-organic-intercalated bentonites modified with transition metal cations, *Environ. Eng. Sci.* **28** (2011) 171. doi: <https://doi.org/10.1089/ees.2010.0213>
69. Bui, T. X., Choi, H., Adsorptive removal of selected pharmaceuticals by mesoporous silica SBA-15, *J. Hazard. Mater.* **168** (2009) 602. doi: <https://doi.org/10.1016/j.jhazmat.2009.02.072>
70. Dordio, A. V., Gonçalves, P., Texeira, D., Candeias, A. J., Castanheiro, J. E., Pinto, A. P., Carvalho, A. J. P., Pharmaceuticals sorption behaviour in granulated cork for the selection of a support matrix for a constructed wetlands system, *Int. J. Environ. Anal. Chem.* **91** (2011) 615. doi: <https://doi.org/10.1080/03067319.2010.510605>